PCCP

Accepted Manuscript

ROYAL SOCIETY OF CHEMISTRY

www.rsc.org/pccp

Journal Name

RSCPublishing

ARTICLE

Coumarin/BODIPY hybrids by heteroatom linkage: versatile, tunable and photostable dye lasers for UV irradiation†

Cite this: DOI: 10.1039/x0xx00000x

Received 00th January 2012,
Accepted 00th January 2012

DOI: 10.1039/x0xx00000x

www.rsc.org/

I. Esnal,[a] G. Duran-Sampedro,[b] A. R. Agarrabeitia,[b] J. Bañuelos,*[,a] I. García-Moreno,[c] M. A. Macías,[d] E. Peña-Cabrera,[d] I. López-Arbeloa,[a] S. de la Moya,*[,b] and M. J. Ortiz [b]

Linking amino and hydroxycoumarins to BODIPYs through the amino or hydroxyl group lets the easy construction of unprecedented photostable coumarin/BODIPY hybrids with broadened and enhanced absorption in the UV spectral region, and outstanding wavelength-tunable laser action within the green-to-red spectral region (~520-680 nm). These laser dyes allow the generation of a valuable tunable UV (~260-350 nm) laser source by frequency doubling, which is essential to study accurately the photochemistry of biological molecules under solar irradiation. The tunability is achieved by selecting the substitution pattern of the hybrid. Key factors are the linking heteroatom (nitrogen vs. oxygen), the number of coumarin units joined to the BODIPY framework and the involved linking positions.

Introduction

Solar ultraviolet (UV) photons constitute one of the most ubiquitous and potent environmental carcinogens. For this reason, a great deal of work concerning the photophysics and photochemistry of the excited states created in key biomolecules (e.g., nucleic acids) upon UV light is being conducted, since such states are at the beginning of the complex chain of biochemical events that culminates in photocarcinogenesis.[1] However, more accurate experiments are urgently needed to understand the dynamics of these excited states, which have been stymied by the lack of suitable laser sources providing efficient, stable and tunable UV radiation within the range of 250-350 nm. An attractive approach to overcome this drawback involves the design of new laser dyes with strong UV absorption and highly efficient and stable emission in the visible (Vis) spectral region (500-700 nm), since it constitutes the only way to generate, efficiently and without undesired re-absorption/re-emission processes, the required tunable UV laser radiation by frequency doubling, and even with ultra-short pumping pulses.

Since it is still difficult to judiciously design single laser dyes fulfilling the mentioned requirements, a powerful strategy is the construction of molecular energy-transfer arrays (coupled or cassette systems) able to achieve efficiently excitation energy transfer from UV-absorbing donors to a covalently-linked Vis-emitting laser dye acting as the acceptor partner. To address this issue, we were prompted to develop unprecedented laser dyes featuring the direct covalent integration of UV-absorbing coumarin (1*H*-chromen-2-one) chromophores into Vis-emitting BODIPY (4,4-difluoro-4-bora-3*a*,4*a*-diaza-*s*-indacene) ones (Fig 1).

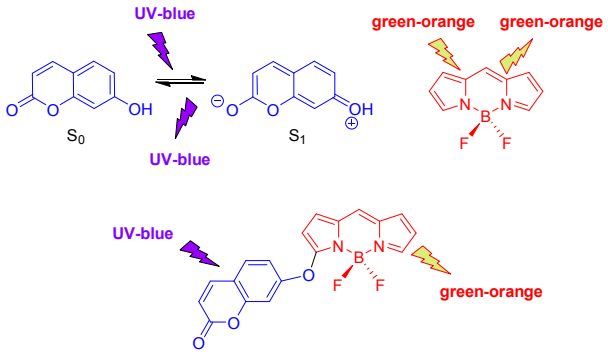

Fig 1. Simple push-pull 7-hydroxycoumarin (blue) and BODIPY (red) chromophores, and a hybrid system based on them.

Coumarins are an interesting family of fluorescent dyes;[2] among them, amino and hydroxycoumarin derivatives (mainly 7-amino and 7-hydroxycoumarins) are especially significant because their photophysical signatures are ruled by internal charge transfer (ICT) upon light absorption (classic push-pull dyes, see Fig 1),[3] which is valuable for developing certain applications (e.g., fluorescent sensing by ICT modulation).[4]

Moreover, simple amino and hydroxycoumarins are characterized by absorbing and emitting in the UV/blue-edge spectral region, taking the emission place with relatively large quantum yield,[5] which has been used for developing blue dye lasers.[2] However, coumarins are not as photostable as other common laser dyes, and they usually undergo bleaching under long UV pumping.[6]

On the other hand, BODIPYs constitute a recognized family of Vis-emitting dyes with noticeable utility in the development of a plethora of photonic tools,[7] due to their excellent photophysical properties, high solubility in organic-solvents improving dyed-material processability (e.g., in the preparation of organic films), and possibility of selective functionalization to finely modulate their physical properties.[7] The usually large molar-absorption coefficients (ε) and high fluorescence quantum yields (ϕ) of BODIPYs have promoted their application as fluorescent dyes for lasing.[7d,8] On the other hand, the characteristic green/orange-edge emission of the BODIPY chromophore should be highly interesting for developing tunable UV lasers by frequency doubling. However, two important drawbacks limit this application: low absorption in the UV spectral region, and small Stokes shifts enabling undesired re-absorption/re-emission processes.

Despite the outstanding and spectrally-complementary photophysical properties of BODIPYs and coumarins, cassettes combining both chromophores are scarce.[9] Thus, the unique two molecular coumarin/BODIPY cassettes described up to now were attained by linking a naked coumarin (non aminated, nor hydroxylated) to a BODIPY cromophore, hence without heteroatom linkage.[9b] On the other hand, non-cassette coumarin/BODIPY hybrids obtained by fusing,[10a] or by linking through a hydrocarbonated spacer[4,10b] both moieties, are described to exhibit interesting photophysical properties (e.g., ICT processes giving place to large Stokes shifts), which are useful for developing certain photonic tools.[4,10] It should be noted that none of these systems have been evaluated as laser dyes. Furthermore, challenging coumarin/BODIPY hybrids involving push-pull amino or hydroxycoumarins covalently linked to the BODIPY chromophore through the amino or hydroxyl heteroatom (note the possibility of ICT processes involving both chromophores) are unknown.

All the above mentioned prompted us to develop the latter coumarin/BODIPY hybrids (e.g., see hybrid based on 7-hydroxycoumarin shown in Fig 1). The main goals of these new molecular dyes should be: (1) a strong UV-blue absorption enabling an efficient green-orange fluorescence and laser, (2) the possibility of emission modulation by tuning ICT processes involving both chromophores[11] and, (3) enhanced photostability of the involved chromophores by its mutual covalent linkage,[8a,8b] which is especially interesting in the case of the photounstable coumarin partner.

Result and discussion

Synthesis. For our purpose, we chose the coumarin/BODIPY structures shown in Fig 2 (i.e., **1dX**, **2**-**4mX** and **2**-**4dX**, with **X** = **A**, **B** or **C**). These structural designs were selected on the basis of synthetic accessibility, and possibility of cassette behavior (**1dX** case) or photophysics modulation by tuning ICT processes (rest of the cases).

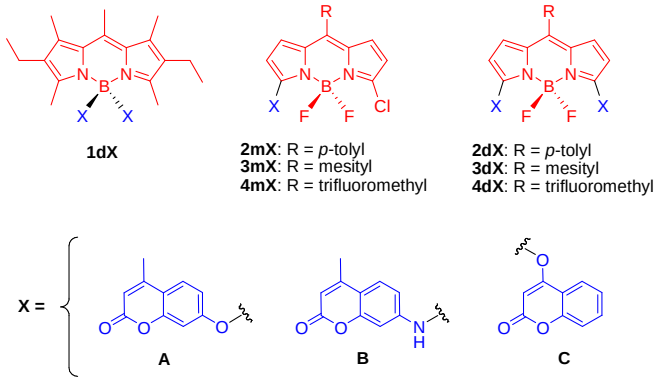

Fig 2. Selected structural designs for coumarin/BODIPY hybrids (up, X = **A**, **B** or **C**), and corresponding coumarin moieties (down).

Dicoumarin-substituted *O*-BODIPY **1dA** was straightforwardly obtained from commercial 2,6-diethyl-1,3,5,7,8-pentamethylBODIPY (PM567, **1**), a known strongly fluorescent green-emitting dye,[12] by $AlCl_3$ promoted substitution of fluorine[8c,13] by the corresponding coumarin (see Fig 3). On the other hand, monocoumarin- and dicoumarin-substituted BODIPYs **2mX** and **2dX**, **3mX** and **3dX**, and **4mX** and **4dX** were obtained by controlled aromatic nucleophilic substitution in 3,5-dichloroBODIPYs (mono or disubstitution),[14] using the corresponding coumarin (**AH**, **BH** or **CH**) as the nucleophile, and 3,5-dichloro-8-(*p*-tolyl)BODIPY (**2**),[14a] 3,5-dichloro-8-mesitylBODIPY (**3**)[15] or 3,5-dichloro-8-(trifluoromethyl)BODIPY (**4**)[14b] as the corresponding starting BODIPY. The latter dihaloBODIPYs were selected on the basis of their synthetic accessibility (Fig 3), and the different stereoelectronic influence of their *meso* groups (R) in the photophysics of the BODIPY chromophore. On the other hand, the coumarins used as nucleophiles in the mentioned halogen (fluorine or chlorine) substitutions were commercial 7-hydroxy-4-methyl-2*H*-chomen-2-one (**AH**), 7-amino-4-methyl-2*H*-chromen-2-one (**BH**) and 4-hydroxy-2*H*-chromen-2-one (**CH**).

Chlorine substitutions on less-activated **2** and **3** (when compared to trifluoromethylated **4**) with less nucleophilic hydroxycoumarins **AH** and **CH** (when compared to aminocoumarin **BH**) required specific base catalysis (see Fig 3). On the other hand, since highly activated **4** was tested to decompose under the employed basic conditions, chlorine substitutions on it (especially by using less activated hydroxycoumarins) were promoted by microwave (MW)

irradiation (see Fig 3). Finally, the synthesis of disubstituted derivatives (**2dX**) required stronger reaction conditions (e.g., longer times; see ESI†) because the involved monosubstituted intermediates (**2mX**) are less activated than the corresponding starting dichloroBODIPYs. This fact is especially significant in the case of the amino derivatives (note the less electron-withdrawing effect of nitrogen when compared with oxygen), and explains the low yield when obtaining **3dB** (null in the case of **2dB**), and the use of MW irradiation for obtaining **4dB** (together with **4mB**) from **4** (see Fig 3).

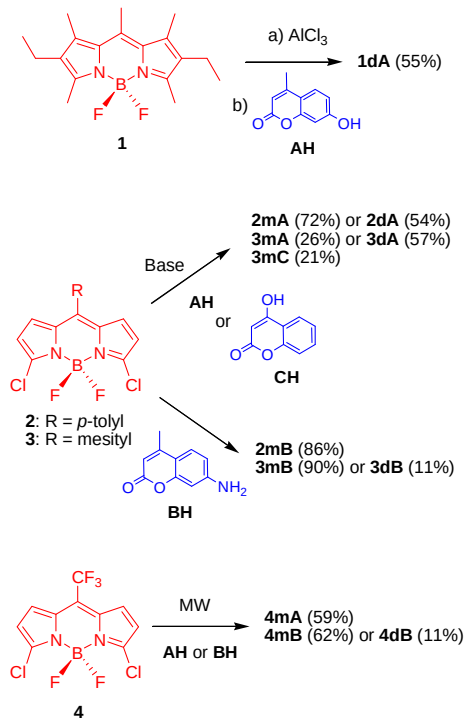

Fig 3. Synthesis of coumarin/BODIPY hybrids (see ESI† for experimental details). Yields into parentheses.

Photophysics. The absorption spectrum of **1dA** was almost the sum of the absorptions of the individual chromophores involved in its molecular structure, as shown by its comparison with the spectra recorded for **1** and **AH** (double concentration for the latter since two coumarin are involved in **1dA**, see Fig 4). Therefore, no noticeable electronic coupling between chromophores exists in **1dA**, at least at its ground state, as it was expected by the role of the linking boron in the BODIPY partner. Indeed, boron is an advisable linking position to develop molecular cassettes based on BODIPY, since it does not participate in the cyanine-like π-system of the BODIPY chromophore, but provides rigidity to it.[16] Theoretical calculations (B3LYP/6-31g) conducted on **1dA** (see ESI†) support also the claimed electronic isolation of chromophores. Thus, the conducted time dependent quantum mechanical simulation (see ESI†) predicts the involvement of molecular orbitals placed exclusively at the coumarin moiety, or at the BODIPY one, for the main electronic transitions associated to each absorption bands (UV and Vis) of **1dA** (see Fig S1 in ESI†). This photophysical result is also supported by electrochemical measurements (see ESI†). Thus, the oxidation and reduction waves recorded in the cyclic voltammogram of **1dA** match almost perfectly with those registered for each individual parent molecules **1** and **AH** (see Fig S2 in ESI†).

In this regime, very weak electronic-coupling limit, the cassette-required selective excitation of chromophores should be feasible. In fact, exciting the BODIPY or the coumarin chromophore in **1dA** (Vis or UV irradiation, respectively) leads to the typical fluorescent BODIPY signature (see Fig 4). Noticeably, the characteristic high quantum yield of the BODIPY chromophore was maintained by UV excitation (ϕ = 82%, see Table S1 in ESI†). Moreover, the observed coumarin-BODIPY intramolecular EET process is highly efficient (approaching the 100%), as demonstrated by the residual emission from the coumarin chromophore, despite its direct excitation (see Fig 4). The short donor-acceptor distance (~5 Å between chromophoric centers, as predicted theoretically) ensures a fast and efficient quenching of the donor by the EET to the acceptor BODIPY.

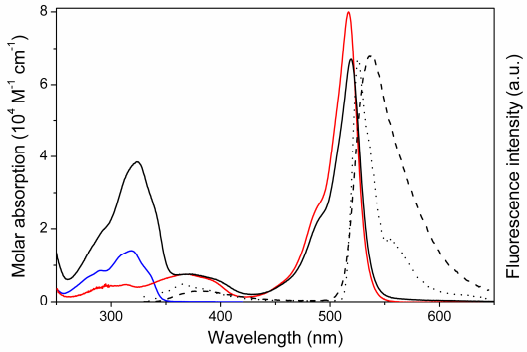

Fig 4. Absorption spectra (bold) of **1dA** (black), **1** (red) and **AH** (blue), and normalized fluorescence spectra of **1dA** (dashed at room temperature; dotted at 77 K‡) upon UV irradiation (325 nm), in ethanol (see ESI† for experimental details).

The EET in **1dA** should take place by the Förster resonance energy-transfer (FRET) mechanism,[17] taking into account: (1) the feasible spectral overlap of the emission transitions of the coumarin donor not only with the UV absorption transitions of the acceptor BODIPY (e.g., $S_0 \rightarrow S_2$),[18] but also, with the Vis ones, although in less extension (see Fig S3 in ESI†); (2) the spatial proximity of the involved chromophores; (3) the lack of orbital overlap avoiding the electronic exchange required by the through-bond energy-transfer (TBET) mechanism,[19] due to the spacing imposed by the tetrahedral boron. Indeed, the EET efficiency of **1dA** was practically the same when decreasing the temperature, even at 77 K, where the electronic-exchange mechanism (an energy-activated process) is virtually nullified.[20] The hypsochromic shift and narrowing of the fluorescence signal upon freezing the sample (Fig 4) is merely due to the low temperature, which lowers the relaxation of the excited state upon irradiation, and hinders the vibrational motion.

Regarding hybrids based on **2** (see Fig 2), their fluorescence response is limited by the rotational free motion of the *p*-tolyl moiety, which drastically enhanced the probability of de-excitation by internal conversion (ϕ = 25% for **2**; see Fig 5, and Table S1 in ESI†).[21] Linking hydroxycoumarin **AH** to BODIPY **2**, to generate hybrid **2mA**, gives rise to a slight decrease in the quantum yield of the BODIPY emission upon Vis irradiation, but without noticeable changes in the shape and position of both the absorption and the emission band (cf. **2** and **2mA** in Fig 5, and in Table S1 in ESI†). However, the replacement of the oxygen linkage of **2mA** by nitrogen in **2mB** decreases significantly the fluorescence (ϕ = 4%), shifts the spectral bands towards the red (mainly in fluorescence, up to ~55 nm), and broadens them (mainly in absorption); (see Fig 5, and Table S1 in ESI†).

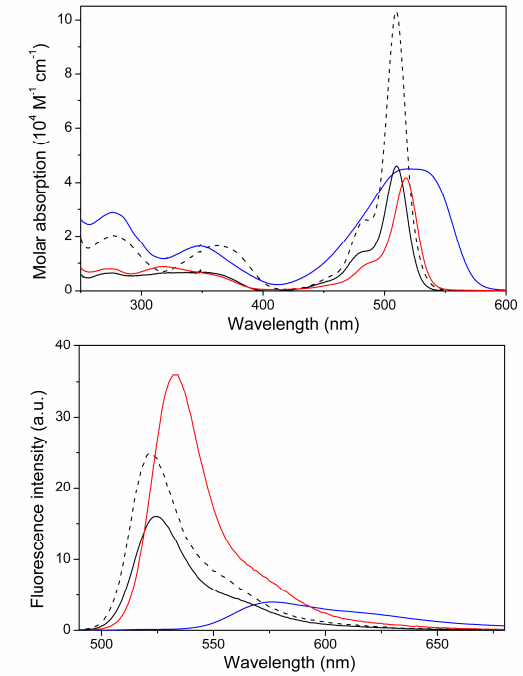

Fig 5. Absorption (up) and fluorescence (down, upon Vis irradiation) spectra of **2** (dashed), **2mA** (black), **2mB** (blue) and **2dA** (red) in ethyl acetate (see ESI† for experimental details).

The mentioned effect observed in **2mB** must result from a strong electronic coupling between the aminocoumarin and the BODIPY due to the involved nitrogen linkage. Additionally, the nitrogen must promote an ICT process, from the coumarin to the BODIPY, due to its known electron-donating ability (note its +K conjugative effect). The ICT must be also favored by the electron-withdrawing effect exerted by the chlorine (strong -I inductive effect) on the BODIPY chromophore. Indeed, the computed frontier orbitals (B3LYP/6-31g; see ESI†) for aminocoumarin-based **2mB** are extended through the whole molecular structure (see Fig S4 in ESI†), which supports an ICT process by the HOMO→LUMO transition. However, the frontier orbitals for hydroxycoumarin-based **2mA**, where the more-electronegative less-conjugative oxygen linkage is involved, shows that the coumarin-BODIPY electronic interaction is much weaker. In fact, the computed frontier orbitals for hybrid **2mA** are mainly located at the BODIPY core, with a small contribution of the oxygen atom (see Fig S4 in ESI†). As consequence of the transfer of electronic density from the coumarin fragment to the BODIPY moiety, not only the fluorescence efficiency decreases, but also the fluorescence lifetimes becomes faster (see data collected in Table S1 in ESI†). The ICT-character of the emitting state implies also an increase of the deactivation rate constants, especially the non-radiative one. Thus, the amino connection induces a more pronounced fluorescence-quenching than the oxygen linkage, due to the less electron-donor character of the latter. Likely, the higher charge-separation promoted in the former case further enhances the non-radiative deactivation probability.

Noticeably, linking an additional **AH** moiety in **2mA**, to generate hybrid **2dA**, boosts the fluorescence quantum up to 36%, producing also a modest red shift in both the absorption and the emission bands (see Fig 5, and Table S1 in ESI†). In agreement with this observation, we have previously demonstrated that symmetrically substituting the 8-(*p*-tolyl)BODIPY chromophore with electronegative atoms at the C3 and C5 BODIPY positions ameliorates the negative effect produced by the aryl motion.[21] Noteworthy, the time dependent simulations of **2**, **2mA**, **2mB** and **2dA** (see Table S2 in ESI†) predict also the observed shifts of the absorption bands as consequence of an increase in the HOMO energy. These agreements of the theoretical predictions with the experimental findings confirm the goodness of the conducted computations.

Although hybrids **2mA**, **2mB** and **2dA** are not able to work as real cassettes because the excitation energy is truly delocalized over both BODIPY and coumarin moieties, especially in nitrogen-linked **2mB** where the electron coupling is more important (cf. frontier orbitals in Fig S4 in ESI†), the UV irradiation gives rise to the same Vis emission observed upon Vis irradiation, without detecting emission signal from the coumarin. However, the observed EET cannot be adequately described by a FRET mechanism, due to the demonstrated high electronic interaction between coumarin and BODIPY moieties (highlighted also by the noticeable different absorption spectra for hybrids and corresponding individual chromophores; e.g., cf. the Vis absorptions of **2mB** and **2** in Fig 5). Thus, the EET observed in these hybrids really lies in a coherent process, where the excitation oscillates back and forth between the donor coumarin and the acceptor BODIPY. In these cases, where operates the electronic mechanism (strong coupling limit), the EET process is extremely fast and efficient.

Restricting the conformation motion of the phenyl ring in *meso*-arylBODIPYs, via the sterical hindrance induced by *ortho* methyl groups in the aryl moiety, is known to ameliorate the BODIPY fluorescence by decreasing the probability of non-radiative deactivation pathways (cf. **2** and **3** in Table S1 in ESI†). Thus, mesityl-based hydroxycoumarin hybrids **3mA** and **3dA** are more fluorescent than the corresponding *p*-tolyl analogues **2mA** and **2dA**. Indeed, the fluorescence quantum

yields of **3mA** and **3dA** are similar to the obtained for parent **3** (higher than 90%; see Fig 6 and Table S1 in ESI†). The same effect is observed when the 7-hydroxycoumarin moiety of **3mA** is substituted by the 3-hydroxycoumarin moiety in **3mC** (see Table S1 in ESI†). However, the strong electronic interaction provided by the nitrogen linkage, when compared with the oxygen one, makes the aminocoumarin-based **3mB** to lose fluorescence ability (ϕ = 7%), probably due to the same ICT process invoked for **2mB**. Indeed, the absorption band of **3mB** is broader, the Stokes shift is larger, and the fluorescence lifetimes are shorter (cf. Figures 5 and 6; see Table S1 in ESI†) than those recorded for **2mB**, due to the higher electronic interaction provided by the nitrogen linkage.

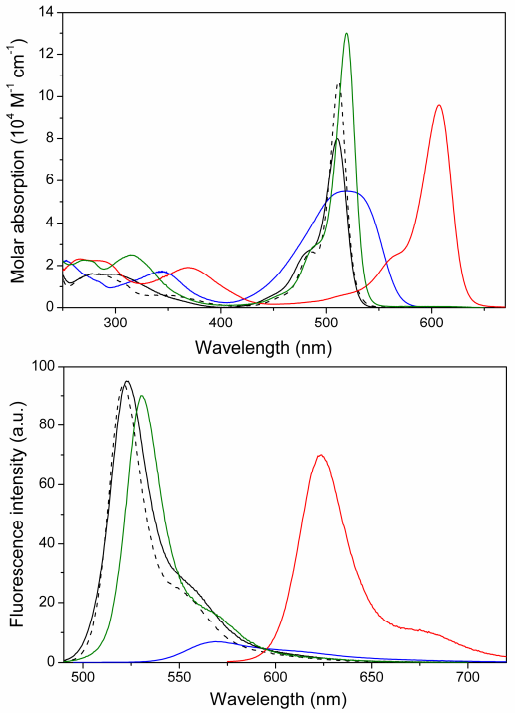

Fig 6. Absorption (up) and fluorescence (bottom, upon Vis irradiation) spectra of **3** (dashed), **3mA** (black), **3mB** (blue) and **3dA** (green) and **3dB** (red) in ethyl acetate (see ESI† for experimental details).

Switching off the ICT process of **3mB**, by introducing a second unit of aminocoumarin to generate **3dB** (note the suppression of the chlorine electronic effect), boosts the fluorescence efficiency (ϕ = 70%; see Fig 6 and Table S1 in ESI†). Noticeably, a deep red shift of both the absorption and emission spectral bands is now observed, recovering such bands the typical narrow shape (vibrational resolution) and Stokes shift of parent **3** (cf. **3**, **3mB** and **3dB** in Fig 6, and in Table S1 in ESI†). This spectral shift was properly predicted by the time dependent simulation also (see Table S2 in ESI†). All these data demonstrate the lack of ICT in **3dB**, as well as the existence of an extended conjugation involving coumarins and BODIPY (see Fig S5 in ESI†). Once again, the UV irradiation of **3dB** was tested to produce the same Vis emission that the obtained by Vis irradiation, showing that this coumarin/BODIPY hybrid could be a promising UV-pumped lasing dye with efficient emission in the orange-edge of the red region (623 nm, see Fig 6) and, therefore, a promising UV-emitting lasing dye (ca. 310 nm) by frequency doubling.

A clear experimental proof of the strong electronic interaction between BODIPY and coumarin moieties in hybrids **3dA** and **3dB** is provided by their electrochemical behavior when compared with the exhibited by parent **3** in the same conditions (see Fig 7). Thus, the oxidation potential decreases noticeably from 1.70 V for **3** (irreversible process), to 1.18 V and 0.63 V for **3dA** and **3dB**, respectively (reversible processes; a second oxidation wave at 1.13 V is additionally detected for **3dB**). Moreover, it is observed that the lower the oxidation potential, the closer are the cathodic and anodic peaks (see Fig 7). These results suggest that the HOMO energy, which is related with the oxidation ability, is significantly higher for the hybrids, as consequence of the electronic coupling. Therefore, the absorption energy gap, which is related with the separation between the cathodic and anodic peaks, is also significantly lower for the hybrids, in agreement with both the observed absorption red-shifts (see Fig 6) and the computational predictions (see Table S2 in ESI†).

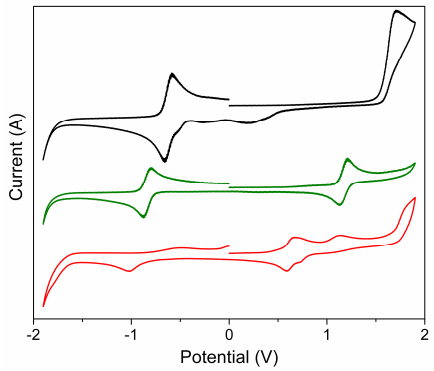

Fig 7. Cyclic voltammograms of **3** (black), **3dA** (green) and **3dB** (red) in acetonitrile (see ESI† for experimental details).

Regarding hybrids based on **4**, their photophysics are characterized by the marked red-shift of the spectral bands imposed by the *meso* trifluoromethyl group (cf. **2**, **3** and **4** in Table S1 in ESI†). Thus, the strong -I inductive effect exerted by the *meso* trifluoromethyl group must stabilize preferently the LUMO state, since it is characterized by a high electronic density at the *meso* position, and differently to that occurring at the HOMO, where a node is placed at such position (e.g., cf. the HOMO and LUMO computed for **2** in Fig S4 in ESI†). This fact must decrease the absorption energy gap, as supported by the conducted theoretical simulations (see Table S2 in ESI†), explaining the observed absorption shifts. However, the same effect should also boost undesired ICT processes from the coumarin to the BODIPY, mainly in the case of mono-aminocoumarin-based **4mB**, but also in mono-hydroxycoumarin-based **4mA**. In fact, **4mB** is observed to be

not fluorescent, while **4mA** exhibits less fluorescence (ϕ = 40%) and faster lifetime than parent **4** (see Table S1 in ESI†).

Analogously to **3dB**, the double-aminocoumarin substitution of **4dB** enhances the fluorescence ability by decreasing the probability of the fluorescence-quenching ICT process (note the lack of the ICT-promoting chlorine), as well as pushes the spectral bands deeply toward the red region (cf. **4mA** and **4dB** in Fig 8), by the establishment of an extended conjugation (cf. the computed energy gaps dated in Table S2 in ESI†). It must be noted that the high fluorescence efficiency (ϕ = 70%) of red-emitting (665 nm) **4dB**, joined to the tested viability of both UV or Vis excitation to record the same Vis emission, makes this dye potentially valuable as a red-emitting lasing dye, but also as a UV-emitting one (ca. 330 nm) by frequency doubling.

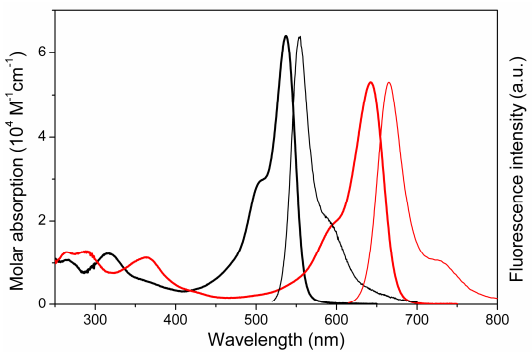

Fig 8. Absorption (bold) and corresponding normalized fluorescence (thin, upon Vis irradiation) of **4mA** (black) and **4dB** (red) in ethyl acetate (see ESI† for experimental details).

The fluorescence efficiency of the studied BODIPY/coumarin hybrids, together with the corresponding parent BODIPYs, is graphically compared in Fig 9, showing that the most promising hybrids for our purpose (lasing by UV pumping) are **3mA**, **3mC**, **3dA**, **3dB** and **4dB**.

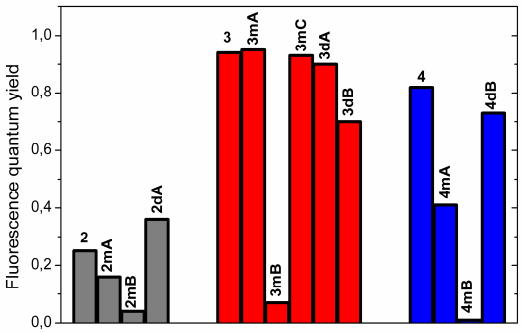

Fig 9. Fluorescence efficiency of BODIPY/coumarin hybrids and corresponding parent BODIPYs in ethyl acetate (data from Table S1 in ESI†).

Laser behavior. With the exception of non-fluorescent **4mB** (see Fig 9), all the obtained coumarin/BODIPY dyes exhibited laser emission either by standard pumping in the UV (355 nm) as in the Vis (532 nm) spectral region. Moreover, coumarin-BODIPY hybridization led to a significant increase in the dye absorption at both pumping wavelengths. This is a key factor from the laser point of view, since it allows reducing significantly the required gain-media concentrations avoiding, consequently, solubility problems, or quenching and/or aggregation processes, all of them with detrimental effect on the laser emission. For instance, hybrid dye **3mB** exhibited molar absorption coefficients of 1.6×10^4 and 5.3×10^4 M^{-1} cm^{-1}, at 355 and 532 nm, respectively, which are well above the coefficients exhibited by parent **3** (0.6×10^4 M^{-1} cm^{-1} at both wavelengths).

Since this work is focused to the development of BODIPY laser dyes able to be UV pumped, we have deeply studied the laser behavior of the obtained coumarin/BODIPY hybrids under laser UV irradiation. To optimize the laser action, we analyzed first the dependence of the laser emission on the dye concentration, keeping constant the rest of the experimental parameters. Ethyl acetate solutions (1 cm path length) with optical densities within the range 1-35 were studied (see ESI†). Thus, under the experimental conditions (transversal excitation and strong focusing of the incoming pumping radiation), the concentration of the dye must be in the millimolar range to ensure total absorption of the pumping radiation over the first millimeter at most of the sample solution, in order to obtain an emitted beam with near-circular cross section optimizing the lasing efficiency, which is defined as the ratio between the energy of the laser output and the pumping energy incising on the sample surface.

Broad-line-width laser emission, with pump threshold energy of ~0.6 mJ, divergence of 5 mrad and pulse duration of 8 ns full width at half maximum (FWHM), was obtained from all the fluorescent hybrid dyes when placed in a simple plane-plane non-tunable resonator. The lasing properties recorded at the optimal concentration for the studied coumarin/BODIPY hybrids and parent BODIPYs are shown in Table 1, showing good correlation with their photophysical properties: the higher the fluorescence quantum yield, the higher is the lasing efficiency; the longer the fluorescence wavelength, the "redder" is the lasing emission; the lower the non-radiative rate constant, the higher is the lasing photostability.

Hybrid dyes based on 3,5-dicoumarin-substituted BODIPY and involving oxygen linkers (**2dA** and **3dA**) achieved laser efficiencies up to 51%, which are much higher than those reached by the corresponding unsubstituted parent dyes **2** and **3** (see Table 1). In fact, the laser efficiency of **3** was poor under the selected laser conditions (28%), whereas **2** and **4** did not exhibit laser emission, but for different reasons. Thus, while the laser behavior of **2** is due to its low fluorescence yield (see Fig 9) preventing laser action, the absence of laser emission from **4** is only caused by its low absorption at the selected pumping UV wavelength. Thus, when **4** is pumped in the Vis region at

532 nm, efficient laser emission (68%) centered at 600 nm is recorded.

Table 1. Lasing properties of coumarin/BODIPY hybrids and parent BODIPY dyes in ethyl acetate solution under transversal UV pumping at 335 nm (see ESI† for experimental details).

Dye	[c]/mM [a]	Eff. (%) [b]	λ/nm [c]	I_n (%) [d]	n/1000 [e]
1	12	20	575	0	6
1dA	2	45	565	25	50
2 [f]	-	-	-	-	-
2mA	1	21	552	20	50
2mB	1	14	610	0	50
2dA	1	35	562	35	50
3	12	22	590	0	50
3mA	2	46	555	40	50
3mB	1	8	615	20	50
3mC	2	45	540	55	50
3dA	2	51	575	55	50
3dB	1	25	645	30	50
4 [f]	-	-	-	-	-
4mA	1	30	615	35	50
4mB [f]	-	-	-	-	-
4dB	1	40	680	55	50

[a]Dye concentration optimizing its laser action in ethyl acetate solution. [b]Lasing efficiency, as the ratio between the energy of the laser output and the pump energy incident on the sample surface. [c]Peak wavelength for the laser emission. [d]Intensity decay for the laser-induced fluorescence emission after n pumping pulses at 10 Hz repetition rate, and measured as $100(I_n/I_0)$ with I_0 being the initial intensity and I_n the after n pulses. [e]Number of pumping pulses. [f]Absence of laser emission under any lasing condition at 335 nm.

In the case of coumarin/**3** hybrids, it must be highlighted the high laser efficiency recorded for the oxygen-linked monocoumarin hybrids **3mA** and **3mC** (ca. 45%; see Table 1), which agrees well with their high fluorescence quantum yields (95% and 93%, respectively, see Fig 9). More surprising was the peculiar behavior of other monocoumarin hybrids, such as **2mA**, **2mB** and **3mB**, because although they exhibited very low fluorescence quantum yields (4%, 16% and 7%, respectively; see Fig 9), they not only presented laser emission but also with laser efficiencies as high as 21% (see Table 1). This fact can be explained by the ICT-character of the emitting states of these hybrids (see Photophysics section), leading to: (a) high Stokes shift (up to 1700 cm^{-1}), which reduces re-absorption/re-emission processes and, thus, their deleterious effect in the laser action; (b) very short fluorescence lifetimes (below to 0.28 ns), which lead to radiative-rate constants similar to those observed for the other hybrid dyes; and (c) high dipole moments allowing the molecular alignment with respect to the polarization of the exciting laser beam to enhance the emission efficiency of the media.[22] The combination of all these factors in the same molecule (see Table S1 in ESI†) is the origin of the unique lasing properties exhibited by these hybrids.

Depending on the number and position of coumarin units joined to BODIPY framework as well as on the nature of the linking heteroatom, the wavelength of the laser emission shifts towards the blue or towards the red with respect to the corresponding parent (unsubstituted) BODIPY. For instance, in the case of hybrids based on **3**, hydroxycoumarin hibrydization (**3mA**, **3dA** and **3mC**) leads to noticeable hypsochromic shifts, whereas the aminocoumarin hybridization (**3mB** and **3dB**) does the opposite (i.e., towards the red, see Table 1). Noticeably, the dye series based on **3** enables to reach wavelength-tunable laser action within the green-to-red spectral region (520-660 nm; see Fig 10).

An important parameter for any practical application of the dye lasers is their lasing photostability under repeated pumping. Table 1 collects data on the decrease of the laser-induced fluorescence intensity of the studied coumarin/BODIPY hybrids and their corresponding parent BODIPYs and coumarins, under transversal excitation of capillary containing dye solutions after n pump pulses at 10 Hz repetition rate (see ESI†). It is well-known that coumarins are rather unstable dyes under laser irradiation. In fact, the studied coumarines lost their laser emission completely after just 6000 pump pulses under the selected experimental conditions. However, data in Table 1 demonstrate that the new coumarin/BODIPY hybrids became photostable laser dyes, enhancing significantly the photostability recorded for the corresponding parent BODIPYs.

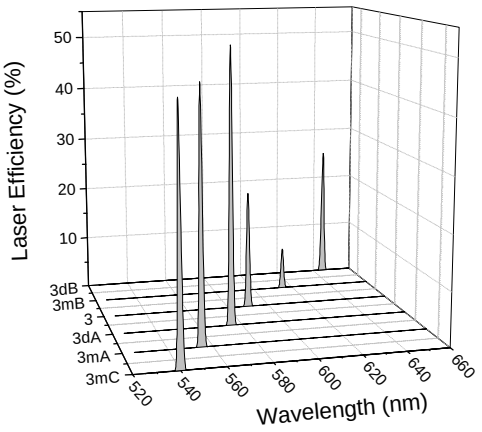

Fig 10. Lasing emission spectra of BODIPY **3** and their couramin/BODIPY hybrids **3mA**, **3mB**, **3mC**, **3dA** and **3dB** (Data from Table 1).

This improvement of the photostability must be related to the excitation energy transfer from the coumarin moieties to the BODIPY core, which allows reducing the rate and extension of the photodegradation processes undergone by coumarins under UV laser irradiation. This behavior is widespread to all the herein developed hybrids, regardless of the acting EET mechanism: via FRET if the coumarins are linked to the BODIPY boron, or by electron coupling if they are directly anchored to the BODIPY chromophore. Once again, the dicoumarin-based hybrids involving oxygen as linking atom

became the most photostable, remaining up to 55% of the initial emission after 50000 pumping pulses. In other words, albeit the photochemically unstable coumarin fragment is directly pumped, the fast transfer of the excitation energy to the BODIPY via electronic coupling provides an optimal laser performance over long exposure periods to irradiation.

Conclusions

Unprecedented coumarin/BODIPY hybrids involving push-pull amino or hydroxycoumarins covalently linked to the BODIPY chromophore through to the amino or hydroxyl coumarin heteroatom could be straightforwardly attained from the corresponding coumarins and BODIPYs by nucleophilic halogen-substitution processes involving the boron or the C3/5 BODIPY position, and adjusting conveniently the reaction conditions to promote and control the substitution reactivity, which is especially important in the case of the hybrids based on 3-coumarin or 3,5-dicoumarin-substituted BODIPY involving oxygen as linkage.

The photophysical signatures of the obtained hybrid dyes are controlled by the type and number of coumarin units, as well as by the involved BODIPY linking position and coumarin linking heteroatom (N or O). Thus, boron is demonstrated to be an optimal linking site to promote BODIPY emission by UV irradiation via FRET, whereas the direct connection of the coumarin to the conjugated framework of the BODIPY chromophore allows a fine modulation of the spectroscopical properties of the dye. Thus, BODIPY double-substitution with aminocoumarins is recommended to avoid undesired ICT phenomena, and achieve bright emission pushed to the red edge, due to a strong resonant interaction, whereas hydroxycoumarins are recommended for enhancing the fluorescence performance.

The developed fluorescent coumarin/BODIPY hybrid dyes undergo lasing with good efficiency and high stability, allowing wavelength finely tunable over a wide range (~520-700 nm). Moreover, their laser action is enhanced when compared with the corresponding parent dyes, and correlates well with their photophysics. The highest lasing efficiencies (up to 51% at 355 nm) were recorded from hybrids based on two hydroxycoumarin and 3,5-disubstituted BODIPY. These hybrids also proved to be the most photostable, with laser emission remaining up to 55% of its initial level after 50000 pump pulses at 10 Hz repetition rate.

The attainment of these novel hybrid dyes based on BODIPY and coumarin, with strong UV absorption and highly efficient and stable laser emission in the green-red spectral region, concerns one of the greatest challenges in the ongoing development of advanced photonic materials with relevant applications. In fact, these organic dyes are the only ones that allow, by frequency doubling, the generation of tunable UV (~260-350 nm) laser radiation with ultra-short pulses. Radiation with these characteristics is essential to analyze accurately the photochemistry of biological molecules, as important as nucleic acids, trying to understand their stability under solar radiation, since their excited states are known to be involved at the beginning of the complex biological events that culminates in photodamage, including photocarcinogenesis, a growing human health problem.

Acknowledgements

Financial support from Spain (MINECO: MAT2010-20646-C04-01, 02 and -04) and Mexico (DAIP: 2014, and CONACyT: 123732I) is gratefully acknowledged. I.E. thanks Gobierno Vasco for a research contract (IT339-10). G.D.-S. thanks MINECO for a predoctoral FPI grant.

Notes and references

[a] *Depto. de Química Física, Universidad del Pais Vasco-EHU, Apartado 644, 48080, Bilbao, Spain. E-mail: jorge.banuelos@ehu.es*
[b] *Depto. de Química Orgánica I, Facultad de CC. Químicas, Universidad Complutense de Madrid, Ciudad Universitaria s/n, 28040, Madrid, Spain. E-mail: santmoya@ucm.es.*
[c] *Depto. de Sistemas de Baja Dimensionalidad, Superficies y Materia Condensada, Instituto de Química-Física "Rocasolano", C.S.I.C., Serrano 119, 28006, Madrid, Spain.*
[d] *Depto. de Química, Universidad de Guanajuato, Col. Noria Alta s/n, Guanajuato, 36050, Mexico.*

† Electronic Supplementary Information (ESI) available: General experimental details, synthetic procedures and characterization data, Figs S1-S5, Tables S1-S2, as well as copies of the NMR spectra recorded from new compounds. See DOI: 10.1039/b000000x/

1 For example, see: C. E. Crespo-Hernández, B. Cohen, P. M. Hare and B. Kohler, *Chem. Rev*., 2004, **104**, 1977.
2 (*a*) *Dye Lasers*, 3rd. Ed, F. P. Schäfer (Ed.), Springer-Verlag, New York, 1990; (*b*) *Dye Laser Principles*, F. J. Duarte and L. W. Hillman (Eds.), Academic, New York, 1990; (*c*) F. López Arbeloa, I López Arbeloa and T. López Arbeloa, *Handbook of Advanced Electronic and Photonic Materials and Devices*, vol. 7, H. S. Nalwa (Ed.), Academic Press. San Diego, 2001; (*d*) F. J. Duarte, *Tunable Laser Optics*, Elsevier Academic, New York, 2003.
3 (*a*) J. Wang, S. Qian and J. Cui, *J. Org. Chem.*, 2006, **71**, 4308; (*b*) G. Signore, R. Nifosi, L. Albertazzi, B. Storti and R. Bizarri, *J. Am. Chem. Soc.* 2010, **132**, 1276.
4 (*a*) S. Lin and W. S. Struve, *Photochem. Photobiol*. 1991, **54**, 361; (*b*) X. Cao, W. Lin, Q. Yu and J. Wang, *Org. Lett.* 2011, **13**, 6098; (*c*) Y. Qian, B. Yang, Y. Shen, Q. Du, L. Lin, J. Lin and H. Zhu, *Sensor. Actuat. B-Chem.*, 2013, **182**, 498; (*d*) A. K. Bhoi, S. K. Das, D. Majhi, P. K. Sahu, A. Nijamudheen, Anoop N., A. Rahaman and M. Sarkar, *J. Phys. Chem. B* 2014, **118**, 9926; (*e*) D. Majhi, S. K. Das, P. K. Sahu, S. M. Pratik, A. Kumar and M. Sarkar, *Phys. Chem. Chem. Phys*. 2014, **16**, 18349.
5 (*a*) B. Wagner, *Molecules*, 2009, **14**, 210; (*b*) X. Liu, Z. Xu and J. M. Cole, *J. Phys. Chem. C.* 2013, **117**, 16584.
6 (*a*) G. Jones II, W.R. Jackson, C.-Y. Choi and W. R. Bergmark, *J. Phys. Chem.*, 1985, **89**, 294; (*b*) S. C. Guggenheimer, J. H. Boyer, K. Thangaraj, M. P. Shah, M. L. Soong and T. G. Pavlopoulos, *Appl. Opt*., 1993, **32**, 3942.
7 (*a*) A. Loudet and K. Burgess, *Chem. Rev*., 2007, **107**, 4891; (*b*) G. Ulrich, R. Ziessel and A. Harriman, *Angew. Chem. Int. Ed*., 2008, **47**,

1184; (*c*) F. L. Arbeloa, J. Bañuelos, V. Martínez, T. Arbeloa and I. López Arbeloa, *Trends Phys. Chem.*, 2008, **13**, 101; (*d*) M. Benstead, G. H. Mehl and R. W. Boyle, *Tetrahedron*, 2011, **67**, 3573; (*e*) N. Boens, V. Leen and W. Dehaen, *Chem. Soc. Rev.*, 2012, **41**, 1130; (*f*) A. Kamkaew, S. H. Lim, H. B. Lee, L. V. Kiew, L. Y. Chung and K. Burgess, *Chem. Soc. Rev*., 2013, **42**, 77; (*g*) A. Bessette and G. S. Hanan, *Chem. Soc. Rev.*, 2014, **43**, 3342; (h) H. Lu, J. Mack, Y. Yang and Z. Shen, *Chem. Soc. Rev.*, 2014, **43**, 4778.

8 (*a*) Y. Xiao, D. Zhang, X. Qian, A. Costela, I. García-Moreno, V. Martín, M. E. Pérez-Ojeda, J. Bañuelos, L. Gartzia, and I. López-Arbeloa, *Chem. Commun.*, 2011, **47**, 11513; (*b*) L. Gartzia-Rivero, H. Yu, J. Bañuelos, I. López-Arbeloa, A. Costela, I. García-Moreno and Y. Xiao, *Chem. Asian J.*, 2013, **8**, 3133; (*c*) G. Durán-Sampedro, A. R. Agarrabeitia, L. Cerdán, M. E. Pérez-Ojeda, A. Costela, I. García-Moreno, I. Esnal, J. Bañuelos, I. López Arbeloa and M. J. Ortiz, *Adv. Funct. Mat.*, 2013, **23**, 4195; (*d*) G. Durán-Sampedro, I. Esnal, A. R. Agarrabeitia, J. Bañuelos, L. Cerdan, I. García-Moreno, A. Costela, I. López Arbeloa and M. J. Ortiz, *Chem. Eur. J.*, 2014, **20**, 2646.

9 (*a*) R. C. A. Keller, J. R. Silvius and B. De Kruijff, *Biochem. Biophys. Res. Commun*., 1995, 508; (*b*) Y. Zhao, Y. Zhang, X. Lu, Y. Liu, M. Chen, P. Wang, J. Liu and W. Guo, *J. Mat. Chem.*, 2011, **21**, 13168.

10 (*a*) A. Y. Bochkov, I. O. Akchurin, O. A. Dyachenko and V. F. Traven, *Chem. Commun.*, 2013, **49**, 11653; (*b*) Z. Yang, Y. He, J.-H. Lee, N. Park, M. Suh, W.-S. Chae, J. Cao, X. Peng, H. Jung, C. Kang and J. S. Kim, *J. Am. Chem. Soc*., 2013, **135**, 9181.

11 BODIPYs are known to undergo ICT processes with groups at the C3/5 position. For example, see: (*a*) X. Peng, J. Du, J. Fan, J. Wang, Y. Wu, J. Zhao, S. Sun and T. Xu, *J. Am. Chem. Soc.*, 2007, **129**, 1500; (*b*) E. Deniz, G. C. Isbasar, Ö. A. Bozdemir, T. L. Yildirim, A. Siemiarczuk and E. U. Akkaya, *Org. Lett.*, 2008, **10**, 3401.

12 F. López Arbeloa, J. Bañuelos, V. Martínez, T. Arbeloa and I. López Arbeloa, *Int. Rev. Phys. Chem*., 2005, **24**, 339.

13 (*a*) C. Tahtaoui, C. Thomas, F. Tohmer, P. Klotz, G. Duportail, Y. Mèly, D. Bonnet and M. Hibert, *J. Org. Chem.*, 2007, **72**, 269; (*b*) E. M. Sánchez-Carnerero, F. Moreno, B. L Maroto, A. R. Agarrabeitia, M. J. Ortiz, B. G. Vo, G. Muller and S. de la Moya, *J. Am. Chem. Soc*., 2014, **136**, 3346.

14 (*a*) T. Rohand, M. Baruah, W. Qin, N. Boens and W. Dehaen, *Chem. Commun*., 2006, 266; (*b*) L. Li, B. Nguyen and K. Burgess, *Bioorg. Med. Chem. Lett.*, 2008, **18**, 3112; (*c*) Y. A. Volkova, B. Brizet, P. D. Harvey, A. D. Averin, C. Goze and F. Denat, *Eur. J. Org. Chem*., 2013, 4270; (*d*) E. M. Sánchez-Carnerero, F. Moreno, B. L. Maroto, A. R. Agarrabeitia, J. Bañuelos, T. Arbeloa, I. López-Arbeloa, M. J. Ortiz and S. de la Moya, *Chem. Commun*. 2013, **49**, 11641.

15 T. Sakida, S. Yamaguchi and H. Shinokubo, *Angew. Chem. Int. Ed.*, 2011, **50**, 2280.

16 For example see: (*a*) C. Goze, G. Ulrich and R. Ziessel, *J. Org. Chem*., 2007, **72**, 313; (*b*) M. A. H. Alamiry, J. P. Hagon, A. Harriman, T. Bura and R. Ziessel, *Chem. Sci.*, 2012, **3**, 1041; (*c*) A. Kaloudi-Chantzea, N. Karakostas, F. Pitterl, C. P. Raptopoulou, N. Glezos and G. Pistolis, *Chem. Commun*., 2012, **48**, 12213; (*d*) N. Karakostas, I. M. Mavridis, K. Seintis, M. Fakis, E. N. Koini, I. D. Petsalakis and G. Pistolis, *Chem. Commun*., 2014, **50**, 1362; (*e*) E. M. Sánchez-Carnerero, L. Gartzia-Rivero, F. Moreno, B. L. Maroto, A. R. Agarrabeitia, M. J. Ortiz, J. Bañuelos, I. López-Arbeloa and S. de la Moya, *Chem. Commun*., 2014, **50**, 12765.

17 (*a*) T. Förster, *Dicuss. Faraday Soc*., 1959, **27**, 7; (*b*) J. Fan, M. Hu, P. Zhan and X. Peng, *Chem. Soc. Rev*., 2013, **114**, 11567.

18 A. Harriman, L. J. Mallon, S. Goeb, G. Ulrich and R. Ziessel, *Chem. Eur. J*., 2009, **15**, 4553.

19 S. Speiser, *Chem. Rev*., 1996, **96**, 1953.

20 (*a*) J. Iehl, J. F. Nierengarten, A. Harriman, T. Bura and R. Ziessel, *J. Am. Chem. Soc*., 2012, **134**, 988; (*b*) D. Bai, A. C. Benniston, J. Hagon, H. Lemmetyinen, N. V. Tkachenko, W. Clegg and R. W. Harrington, *Phys. Chem. Chem. Phys*., 2012, **14**, 4447.

21 G. Duran-Sampedro, A. R. Agarrabeitia, I. García-Moreno, A. Costela, J. Bañuelos, T. Arbeloa, I. López Arbeloa, J. L. Chiara, M. J. Ortiz, *Eur. J. Org. Chem*., 2012, 6335.

22 L. Cerdán, A. Costela, I. García-Moreno, J. Bañuelos and I. López-Arbeloa, *Laser Phys. Lett*., 2012, **9**, 426.